Sterile neutrino dark matter, matter-antimatter separation, and the QCD phase transition

Mikhail Shaposhnikov[1,*] and Alexey Yu Smirnov[2,†]

[1]*Institute of Physics, École Polytechnique Fédérale de Lausanne (EPFL), CH-1015 Lausanne, Switzerland*
[2]*Max-Planck-Institut für Kernphysik, Saupfercheckweg 1, 69117 Heidelberg, Germany*

(Received 15 October 2023; revised 24 May 2024; accepted 15 August 2024; published 10 September 2024)

The Universe may contain sufficiently small size matter-antimatter domains at temperatures of a few hundred MeV, without violating the success of big bang nucleosynthesis. We demonstrate that this possibility enhances the keV scale sterile neutrino production and may lead to its abundance consistent with the observable energy density of dark matter (DM). Assuming that the quantum chromodynamics (QCD) phase transition is of the first order we argue that it may lead to the separation of matter and antimatter, creating temporarily macroscopic domains occupied by hadronic matter and quark-gluon plasma. In these domains an excess of baryons over antibaryons and vice versa largely can exceed the average baryon and lepton asymmetries of the Universe. We discuss several scenarios of matter-antimatter separation at the QCD phase transition and the production of DM sterile neutrinos in each of them. One of the possibilities requires the presence of lepton asymmetry of the Universe, which can be smaller than that needed for the DM correct abundance in the homogeneous case. Another, the more speculative one, is related to the Omnes phase transition and does not require lepton asymmetries.

DOI: 10.1103/PhysRevD.110.063520

I. INTRODUCTION

The motivation for the sterile neutrino dark matter (DM) candidate [1,2] stems from discovery of neutrino oscillations [3–17]. The simplest and most natural way to get nonzero neutrino masses is to add to the Standard Model several (at least two) right-handed neutrinos (or, what is the same, Majorana fermions or heavy neutral leptons-HNLs) [18–22]. These particles have Yukawa couplings with the Higgs boson and leptonic doublets, which generate the active neutrino masses via the see-saw mechanism. If the number of HNLs is three (the same as the number of fermionic generations in the Standard Model) this model, known as the minimal type I seesaw model or the νMSM (neutrino minimal Standard Model) [23,24], is capable of explaining simultaneously the Dark Matter (in terms of the lightest HNL—N_1 with the mass in the keV range), and also neutrino masses and baryon asymmetry of the Universe coming about because of heavier HNLs $N_{2,3}$, addressing thus all experimental drawbacks of the SM. The keV sterile neutrinos do not contribute to the masses of light neutrinos, which allows us to fix the absolute scale of active neutrino masses [23] within the νMSM.

In the νMSM, the DM sterile neutrinos are most effectively produced via mixing with active neutrinos in reactions with other particles of the SM, such as $l^+l^- \to \nu N_1$, at temperatures of a few hundred MeV.[1] In the case of small lepton asymmetries of the Universe (the Dodelson-Widrow mechanism [1]), the required mixing angle is in contradiction with x-ray[2] and structure formation constraints.[3]

We define lepton asymmetry as $\Delta_L = L/s$, where L is the density of the total lepton number and s is the entropy density. If the asymmetry is much larger than the baryon asymmetry [36,37], and furthermore

$$\Delta_L \gtrsim L_{\rm crit} \equiv 6.6 \times 10^{-5}, \tag{1.1}$$

then the production of the sterile neutrinos is resonantly enhanced according to the Shi-Fuller mechanism [2] and all the constraints mentioned above can be satisfied (for a review see [35]). The quantities Δ_L and $L_{\rm crit}$ in Eq. (1.1) are

*Contact author: mikhail.shaposhnikov@epfl.ch
†Contact author: smirnov@mpi-hd.mpg.de

[1]The DM sterile neutrino may also be created in the processes including physics beyond the νMSM. The proposals include the decays of extra scalar particles [25,26], higher-dimensional operators [27], Einstein-Cartan 4-fermion gravitational interaction [28], left-right symmetric theories [29] etc.

[2]N_1 is unstable and can decay as $N_1 \to \gamma\nu$, producing a narrow X-ray line that can be seen by x-ray telescopes [30–32]. Evidence for such a line at 3.5 keV which would correspond to decays of 7 keV DM sterile neutrino was reported in [33,34]. It remains to be seen if this line indeed corresponds to the radiative decay of DM particles.

[3]The free streaming length of N_1 admitted by the x-ray constraints is too large and contradicts to the cosmological Lyman-α forest data, for a review see [35].

taken at a temperature 4 GeV, and it is assumed that the lepton numbers of different generations can only be changed due to the mixing with DM sterile neutrino (or, in other words, that the processes with $N_{2,3}$ of the νMSM are irrelevant). The number $L_{\rm crit}$ depends on the flavor composition of the lepton asymmetry, on the sterile neutrino mixing angle θ, and on the mass of the DM sterile neutrino [36,37]. The specific value of $L_{\rm crit}$ given above in (1.1) corresponds to $L_e = L_\mu = L_\tau = L/3$, $M_1 = 7$ keV, and $\theta^2 = 5 \times 10^{-11}$ [37].

The lepton asymmetries of this magnitude can indeed be produced in the νMSM, albeit in a fine-tuned domain of the parameter space leading to strong mass degeneracy between heavier HNLs N_2 and N_3 [38–40].

To the best of our knowledge, in all approaches to sterile neutrino production proposed so far, the Universe was taken to be homogeneous and isotropic at the relevant temperatures of the order of 200 MeV. However, this is a mere assumption. The success of the big bang nucleosynthesis (BBN) indicates that this was very likely to be the case at smaller temperatures $T \sim 1$ MeV, but the inhomogeneities at $T \sim 200$ MeV with a size as large as few meters are admitted [41], as they dissipate before the BBN starts through the combined action of neutrino inflation and neutron diffusion [42–46]. Moreover, even the existence of matter-antimatter domains with a baryon-to-entropy ratio of the order of one (or minus one) is allowed, provided their size is smaller than the neutron diffusion length at the BBN epoch.

The presence of these domains may change considerably the sterile neutrino DM abundance and their momentum distribution, important for structure formation. Indeed, even though the average baryon asymmetry of the Universe is small, it can be large locally, leading to the resonant production of sterile neutrinos. Furthermore, the resonance will occur for the left chirality of sterile neutrinos in one type of domain, and with right chirality in another, producing the chiral symmetric DM, contrary to the resonance production in the homogeneous situation.

How the matter-antimatter domains can appear in the Universe? One of the mechanisms suggested in the literature a while ago is associated with a possible existence of stochastic hypermagnetic fields at temperatures above the sphaleron freeze-out [47] (see also [48,49]). The electroweak anomaly converts the hypermagnetic fields into baryons and thus leads to an inhomogeneous Universe with matter-antimatter domains. Yet another possibility to have matter-antimatter domains appears in theories with two sources of CP-violation—spontaneous and intrinsic [50]. Also, the matter-antimatter domains may appear in inhomogeneous baryogenesis, described in [51,52].

Our current work gives yet another example, associated with the possible first-order QCD phase transition if it occurs. We will show that in the scenario with matter-antimatter separation at the first-order QCD phase transition, the sterile neutrino DM production may be enhanced considerably. The enhancement can be efficient even if the asymmetry is small $\Delta_L < L_{\rm crit}$, or even absent, $\Delta_L = 0$ if the Omnes type picture of the separation (discussed in Sec. II C) is correct. Though we concentrate on these specific mechanisms of matter-antimatter separation at the QCD epoch, our findings about sterile neutrino DM generation are universal and applicable also to other possibilities, mentioned above. In most numerical estimates, we take $M_1 = 7$ keV and $\theta^2 = 5 \times 10^{-11}$, but the equations we present are valid for the other choice of parameters as well.

To sum up, the aim of the present paper is twofold. First, assuming that the QCD phase transition indeed takes place, we argue that it may lead to temporary matter-antimatter separation, creating macroscopic domains (and "antidomains") with an excess of baryons over antibaryons (and vice versa) substantially exceeding the average baryon and lepton asymmetries of the Universe.

Second, we uncover a new possible consequence of the first-order QCD phase transition, associated with the production of sterile neutrino DM. We will see that the inhomogeneities produced at this transition may facilitate the otherwise suppressed creation of sterile neutrinos. The droplets of QGP rich in baryon number formed at the first order QCD phase transition play a crucial role in the mechanism of sterile neutrino DM production we propose. We will see that the creation of sterile neutrinos via the conversion (oscillations) of ordinary neutrino ν into N_1 inside the droplets may lead to the DM abundance consistent with observations. In addition, after the phase transition, the same type of production processes occur in the hadronic phase inside the lumps with the excess of the baryon number, slowly spreading when the Universe expands. The enhancement of sterile neutrino production is similar to the MSW effect in neutrino oscillations in the medium [53].

The paper is organized as follows. In Sec. II, we consider possible scenarios of matter-antimatter separation at the QCD phase transition. In Sec. II A, we get a glimpse of its possible parameters and get a rough estimate of the average distance between nucleating bubble centres and the probability distribution of the droplets of quark-gluon plasma as a function of their sizes (using the previous studies of the QCD phase transition [54,55]). Section II B discusses the mechanism(s) of matter-antimatter separation in the first-order QCD phase transition. In Sec. III we investigate the sterile neutrino production in the scenarios with matter-antimatter separation. We study first the resonance N production in a homogeneous medium and apply it to Omnes phase transition and QGP droplets of big size. The case of small droplets is considered in Sec. III E. In the last section, we summarize our results.

II. QCD PHASE TRANSITION AND MATTER-ANTIMATTER SEPARATION

There is a common belief that the evolution of the Universe in the framework of the Standard Model of elementary particles is smooth. Potentially, during the Universe cooling after the big bang, one could encounter two phase transitions. The first one is the electroweak phase transition (EWPT) at $T \simeq 160$ GeV passing from the symmetric to the Higgs phase. The second one is the QCD phase transition at $T \simeq 160$ MeV from the quark-gluon plasma to the gas of hadronic states. In both cases, there is no true gauge-invariant local order parameter that can distinguish involved phases, meaning that in general the phase transitions are either absent (smooth cross-over), or are of the first order. A specific choice of parameters of the theory may lead to a second-order phase transition (for example, in the EW case this would happen if the Higgs boson mass were $M_H \approx 73$ GeV [56,57]). For the Standard Model with the Higgs boson heavier than ∼60 GeV and in the QCD, the nature of the phase transitions cannot be identified by the use of perturbation theory, and one has to use nonperturbative methods such as lattice simulations.

The precision study of the EWPT can be done by a combination of perturbative and nonperturbative computations. In the first step, one constructs an effective *three-dimensional purely bosonic theory* containing the gauge bosons of the $\mathrm{SU}(2) \times \mathrm{U}(1)$ group and the Higgs doublet [58]. This effective theory is a lot simpler than the original four-dimensional Standard Model: there are no fermions and no strong SU(3) interactions; moreover, the effective theory is superrenormalizable. All these allow for very accurate lattice simulations. The lattice study of the EW case included (i) the analysis of the first-order transition line existing at small Higgs boson masses, (ii) a comparison of the parameters of the phase transition found on the lattice with the results of perturbation theory in the region of its validity, and (iii) nonperturbative computation of the latent heat, jump of the order parameter, and of the interphase tension. In addition, the analysis of the scaling behavior and critical indexes of the critical point has been carried out. This program led to the conclusion that for the experimentally measured value of the Higgs mass $M_H \approx 125$ GeV, the transition from the symmetric to the Higgs phase in the SM is a smooth crossover [56,57,59] (it would be a first-order phase transition if the Higgs mass were below 73 GeV).[4] Even if the lattice simulations of the EW phase transition missed the very weak first-order phase transition due to the volume or the finite lattice spacing limitations, they can exclude cosmological applications of this phase transition. Indeed, for a 125 GeV Higgs boson the transition temperature (160 GeV) is larger than the sphaleron freeze-out temperature, meaning that it is irrelevant for baryogenesis.

The study of the QCD phase transition is way more complicated. At the temperatures of the order of the confinement scale $\Lambda \sim 200$ MeV, where the phase transition (if any) is expected to take place, the system is strongly coupled, and no three-dimensional effective bosonic description is possible. In addition, there are technical challenges of putting on the lattice nearly massless quarks, such as u or d, and eventually s. Nonetheless, the lattice studies [62–66] reported evidence (considered overwhelming) for the smooth cross-over. Unfortunately, we did not manage to find in the literature the quantitative statement about the confidence level of this evidence and the bounds on the parameters of the phase transition (in the assumption that it happens), such as the latent heat and the interphase tension, important for cosmological applications. Given this uncertainty we take the liberty to assume the QCD phase transition is of the first order and study how it may develop in the early Universe, as was done, for instance, in [67,68]. Intriguingly, the frequencies and spectrum of waves detected by NANOGrav indicate the OCD scale [68,69], giving an extra motivation to consider this possibility.

A. Cosmic separation of phases

Let us assume for the time being that there are just two phases—hadronic and QGP that may coexist in some interval of temperatures $T_- < T < T_+$. A more intricate and very speculative possibility will be discussed in Sec. II C.

We start from a short overview of the previous works on this problem, relevant to us. We assume in what follows that before the QCD phase transition the Universe is homogeneous and contains a tiny baryon asymmetry, $\Delta_B \equiv B/s \simeq 9 \times 10^{-11}$ (B and s are the densities of the baryon number and entropy respectively) and, perhaps, the comparable lepton asymmetry. As was argued by Witten [70] the first-order QCD phase transition may lead to cosmic separation of hadronic and QGP phases. When the universe supercools somewhat below the critical temperature T_c (we take it to be $T_c \simeq 160$ MeV for numerical estimates) the bubbles of new, hadronic phase nucleate. The shock waves originating from the bubble expansion reheat quickly the quark phase up to the critical temperature, and the universe stays at a constant temperature T_c during the sizeable fraction of the Hubble time until the end of the transition. The hadron bubbles grow slowly and roughly with the Hubble rate H. They start to percolate at the moment t_0 when their fraction reaches ∼50% of the space. After that, the situation is reversed—the hadronic phase is dominating, and the droplets with the quark-gluon plasma inside shrink slowly.

This process may lead to the separation of the net baryon number [70]: the droplets with the plasma are much richer

[4]The four-dimensional lattice simulations of the bosonic sector of the EW theory [60,61] confirmed this conclusion.

in baryon number than the baryonic phase, because quarks are lighter than hadrons and the transport of the baryon number over the phase boundary is suppressed [70,71]. It was conjectured in [70] that the baryon asymmetry inside the droplets can be of the order of one at the end of the phase transition.[5] The dynamics of the bubble nucleation in QCD phase transition in this case is mainly determined by the latent heat l and the interphase tension σ. It was considered in detail in [54], and we just give here the main formulas from this article.

First, the Universe is supercooled in the QGP state till temperature T^* (T^* is defined as a moment when the shock fronts originated on the nucleated bubbles start to collide). The amount of supercooling is characterized by

$$x^2 = \left(1 - \frac{T^*}{T_c}\right)^2 \simeq A\left[4\log\left(\frac{2M_0}{T_c}\left(\frac{2\pi v^3}{3A}\right)^{\frac{1}{4}}\right)\right]^{-1}, \quad (2.1)$$

where $M_0 \simeq M_P/(1.66 g^{*\frac{1}{2}})$, $M_P = 1.22 \times 10^{19}$ GeV, $g^* = g^*_w + g^*_{\rm QCD}$ is the number of effectively massless degrees of freedom ($g^*_{\rm QCD}$ corresponds to the QCD degrees of freedom, and g^*_w counts the rest), $v^2 \approx 1/3$ is the sound speed and A is the combination of l and σ,

$$A = \frac{16\pi\sigma^3}{3l^2 T_c}. \quad (2.2)$$

At $T = T_c \simeq 160$ MeV we take, following [72], $g^*_w \simeq 14.25$, $g^*_{\rm QCD} \simeq 10$, leading to $M_0 \simeq 1.4 \times 10^{18}$ GeV and to the horizon size of the Universe $t_H = M_0/T^2 \simeq 10^6$ cm.

The average distance between the nucleated bubbles of the hadronic phase is given by

$$r_0 \simeq t_H \frac{x^3}{A}, \quad (2.3)$$

and the probability distribution of the bubbles on their size r is roughly

$$d\mathcal{P} = \exp\left(-\frac{r}{r_0}\right)\frac{dr}{r_0}. \quad (2.4)$$

After the bubbles start to percolate, the picture is inverted: the hadronic phase becomes dominant, and the droplets of the QGP, having initially the average size $\sim r_0$ will be slowly shrinking and disappear eventually at the end of the phase transition, after the time of the order of the age of the Universe at the QCD phase transition.

A crucial parameter in this picture is the distance between the nucleated bubbles r_0, estimated in [54] as $r_0 \simeq 100$ cm, four orders of magnitude smaller than the horizon size. So, it would be not unreasonable to assume that r_0 is somewhere between 1 cm and 1 m. As we have already mentioned, this scale of inhomogeneities is too small to change the picture of the standard BBN.

If the baryon number is indeed confined inside the droplets of QGP, the baryon number density in the droplets, $n^d_B(t)$, is given by the solution of the equation

$$\frac{\partial n^d_B(t)}{\partial t} = -\frac{3\dot{r}}{r} n^d_B(t), \quad (2.5)$$

leading to the obvious solution

$$n^d_B(t) = n^d_B(t_0)\left(\frac{r(t_0)}{r(t)}\right)^3, \quad (2.6)$$

where $r(t)$ is the time-dependent droplet size, decreasing toward the end of the phase transition and $n^d_B(t_0) = \Delta_B \times s$ is the initial average baryon number density.

Having this basic picture in mind, we now extend it to the case when in addition to tiny baryon asymmetry the universe contains a sizable lepton asymmetry $\Delta_L \equiv L/s$, several orders of magnitude larger than the baryon asymmetry but still small enough to contradict different bounds coming, for instance, from big bang nucleosynthesis (BBN) [73]. The values as large as $\Delta_L \simeq 10^{-4}$ (i.e., million times more than the baryon asymmetry) can be generated, for example, in interactions of heavy neutral leptons (HNLs) of the νMSM below the freeze out of sphaleron transitions, thus having no influence on baryon asymmetry of the Universe [38–40,74,75]. If the lepton asymmetry of the Universe (or its different flavor components) is close to its upper bound imposed by BBN, it can even change the standard cross-over picture of the QCD phase transition converting it to a first-order phase transition [76–78]. We are not going to consider this possibility in our work, since so large lepton asymmetry already ensures the sterile neutrino DM production in the homogeneous situation. Still, the dynamics of the first-order QCD phase transition, in this case, should account for the effects we discuss in the next section.

B. Lepton asymmetry and matter-antimatter separation

For the following discussion, it is important to know the rates of the different weak reactions in the primordial plasma at the time of the QCD phase transition. The electron neutrino mean interaction rate coming from the scattering on leptons is given by [79]

[5]Witten suggested in [70] that the QGP droplets or quark nuggets could be absolutely stable if the baryon number trapped in them is sufficiently large. If true, these objects can serve as valid dark matter candidates. In our work, we do not follow this suggestion and assume, accepting the common lore, that the spectrum of stable states in QCD is standard and is composed of protons and known nuclei.

$$\Gamma_{\nu_e} = \frac{13}{9}\frac{7\pi}{24} G_F^2 T^4 \omega, \tag{2.7}$$

where G_F is a Fermi constant, and ω is the neutrino energy. A similar value is obtained for the muon neutrino. For τ neutrino the rate is somewhat smaller due to the exponential suppression of τ-lepton concentration. The presence of quarks in QGP and mesons and baryons in the hadronic phase changes these estimates (for discussion of hadronic uncertainties see [36,37,80,81]) in an amount irrelevant to the present discussion. For a typical neutrino energy, $\omega \sim 3T_c$ the neutrino mean free path (including their scattering on quarks) is $\lambda_\nu \sim 0.4$ cm, about six orders of magnitude smaller than the horizon size ~10 km at this time.

The rates of quark flavor nonconservation due to reactions of the type $\bar{u}d \to \mu^+\nu_\mu$, $\bar{u}s \to \mu^+\nu_\mu$ in QGP phase, and similar for the electron flavor, is difficult to estimate reliably due to the strong coupling. It is expected that the number of effectively massless degrees of freedom in the QCD plasma at $T_c \sim 160$ MeV goes from $g^*_{\rm free} = 47.5$ (accounting for massless gluons and u, d, and s quarks) to $g^*_{\rm int} \simeq 10$ [72]. As the interaction rate is proportional to the concentration of particles, it is reasonable to expect that the weak mean free path of u and d flavors is some factor ~5 larger than that of neutrinos, $\lambda_{u,d} \sim 2$ cm, and factor ~100 larger for s-quark, accounting for the Cabibbo angle suppression by $\sin^2\theta_c \simeq 0.05$, $\lambda_s \sim 40$ cm. We expect to have similar estimates in the hadronic phase due to reactions of the type $\pi\pi \to \pi\nu e^+$, $\pi K \to \pi\nu\mu^+$ and alike (the rates of 2-body decays of pions and kaons are suppressed either by chirality conservation or by the amount of the available phase space).

The specific numbers for the mean free path given above are not that important in what follows. What is relevant for us is that the transitions between different hadronic flavors are well in thermal equilibrium. In other words, an equilibrium plasma in the vicinity of the QCD phase transition is characterized by five chemical potentials μ_B, μ_i, and μ_Q, corresponding to five conserved numbers: B—baryon number, $L_{e,\mu,\tau}$—three different lepton numbers, and electric charge Q. Imposing the electric neutrality of the QGP plasma, and neglecting for simplicity the masses of the light quarks u, d, s and leptons e, μ and any interactions between them one can easily find in linear order in asymmetries:

$$\frac{\mu_B}{T} = \frac{3B}{T^3}, \quad \frac{\mu_Q}{T} = \frac{3n_{L_e} + 3n_{L_\mu}}{4T^3},$$
$$\frac{\mu_1}{T} = \frac{5n_{L_e} + n_{L_\mu}}{2T^3}, \quad \frac{\mu_2}{T} = \frac{n_{L_e} + 5n_{L_\mu}}{2T^3}, \quad \frac{\mu_3}{T} = \frac{6n_{L_\tau}}{T^3}, \tag{2.8}$$

where n_i are the number densities of the corresponding conserved numbers in the obvious notations. In this approximation, the asymmetries in the number of d and s quarks are the same. If the mass of s-quark is included, this degeneracy is broken. The analogous equations can be derived in the hadronic phase in the noninteracting gas approximation, with the use of baryons and mesons instead of quarks.

These relations show that in the presence of substantial lepton asymmetries $n_{L_i} \gg B$ the asymmetries in the individual quark flavors are of the order of n_{L_i}, rather than B. The importance of lepton asymmetries to the description of the QCD plasma was noted already in [82]. A similar picture arises in the hadronic phase, with excess of protons over antiprotons and mesons over antimesons of the order of lepton asymmetries. The physics of this phenomenon is obvious and is associated with the electric neutrality of the plasma: the equilibrium character of the weak interactions redistributes the leptonic asymmetry between neutrinos and electrically charged leptons, and the asymmetries in hadronic flavors are created to compensate for the charge imbalance.

We are coming now to our main observation. The nonzero and relatively large (of the order of lepton asymmetry) chemical potential μ_Q breaks discrete symmetries C, CP, and CPT that distinguish hadronic matter and antimatter, both in the QGP and hadronic phase. In addition, the mass of the strange quark and masses of strange mesons and baryons are the order of the critical temperature or larger, which breaks the SU(3) flavor symmetry. It is plausible to think that these breakings are transmitted to the interaction of quarks and hadrons with the interphase boundary between the different phases.[6] In the picture of a dilute gas of quarks and hadrons, this would result in a difference between reflection and transmission coefficients for particles carrying baryon and antibaryon numbers. For example, for a quark incident in the QGP phase the probability $\mathcal{P}_r$ of reflection back would be different from that ($\bar{\mathcal{P}}_r$) of the antiquark. Since the interactions between quarks and hadrons are strong, it is conceivable to assume that the CP(T) asymmetry in reflection coefficients $\Delta\mathcal{P} \equiv \mathcal{P}_r - \bar{\mathcal{P}}_r$ is of the order of

$$\Delta\mathcal{P}_0 \simeq \kappa\frac{\mu_Q}{T} \simeq \frac{\kappa L}{2T^3} \simeq 5\kappa\Delta_L, \tag{2.9}$$

where κ is an unknown parameter presumably of the order of one. We used here the entropy density at $T = T_c$, $s \simeq \frac{2\pi^2}{45} g^* T^3$ with $g^* \simeq 24$. The asymmetry $\Delta\mathcal{P}_0$ should be zero if the flavor symmetry were exact, we expect it to behave as m_s^2/T_c^2 for $m_s \to 0$.

[6]Of course, the C and CP-symmetries are also broken by the weak interaction due to Kobayashi-Maskawa CP-violating phase. We do not expect this to play any role in the matter-antimatter separation scenario discussed below since the rate of the weak processes is much smaller than the rate of strong interactions.

In a complete thermal equilibrium, with the domain wall at rest, this dynamical feature does not lead to any substantial consequences: the asymmetries in hadronic flavors in different phases can be found by standard methods of equilibrium thermodynamics (see, e.g., [70] for a sample computation) using the same chemical potentials for conserved charges across the interphase boundary. Now, if the domain wall is moving with velocity $v = \dot{r}$, the difference in reflection probabilities together with nonequilibrium induced by the bubble wall motion will lead to the baryon current J of the order of

$$J \sim -\Delta\mathcal{P}_0 v n_q, \tag{2.10}$$

floating inside the droplets of the QGP (given $|\Delta_L| \gg \Delta_B$ the sign of this current is irrelevant for what follows). Here

$$n_q \simeq g^*_{\rm QCD} n_f = \frac{3\zeta(3)}{4\pi^2} g^*_{\rm QCD} T^3 \simeq 0.9T^3 \tag{2.11}$$

is an estimate of the total density of quarks and antiquarks in the QGP (the zero mass free fermionic concentration is $n_f = 3\zeta(3)/(4\pi^2)T^3$). So, Eq. (2.5) for the baryon number density receives an additional contribution associated with this flux,

$$\frac{\partial n^d_B(t)}{\partial t} = -\frac{3\dot{r}}{r} n^d_B(t) - \dot{r} n_q \Delta\mathcal{P}_0 S/V, \tag{2.12}$$

where $V = 4/3\pi r^3$ and $S = 4\pi r^2$ are the volume and surface of the droplet respectively. The solution of (2.12) reads

$$n^d_B(t) = n^d_B(t_0)\left[\frac{r(t_0)}{r(t)}\right]^3 + \Delta\mathcal{P}_0 n_q \left[\frac{r(t_0)^3}{r(t)^3} - 1\right]. \tag{2.13}$$

For the baryon asymmetry n_b of the bulk exterior to the QGP droplet, corresponding to the hadronic phase, one gets in the full analogy

$$n_b(t) = n^d_B(t_0)\frac{V_0}{V_b} - \Delta\mathcal{P}_0 n_q \left(\frac{V_0}{V_b} - 1\right), \tag{2.14}$$

where V_b is the volume occupied by the hadronic phase, and V_0 is its initial value at the moment of the bubble percolation. Once the size of the droplet at some time t_1 gets just 25% smaller than its initial value, the value of the baryon asymmetry inside the droplet will increase to the value of the order of initial lepton asymmetry, $n^d_B(t_1) \simeq \Delta\mathcal{P}_0 n_q$. This large asymmetry may lead to even higher asymmetry in the reflection coefficients,

$$\Delta\mathcal{P} \simeq \kappa_1 \frac{n^d_B}{n_q}, \tag{2.15}$$

where κ_1 is another unknown parameter, similar to κ. Using Eq. (2.15) in (2.12) one finds that the baryon density inside the QGP droplet increases as

$$n^d_B(t) = n^d_B(t_1)\left[\frac{r(t_1)}{r(t)}\right]^{3+3\kappa_1}, \tag{2.16}$$

reaching the nuclear density at $r(t) \simeq r_0 \mathcal{P}_0^{\frac{1}{3(1+\kappa_1)}}$.

The solutions (2.13) and (2.16) correspond to the matter-antimatter separation. The total baryon number of the Universe does not change but gets unequally distributed in the domains (droplets) occupied by the QGP and hadronic matter, the first type carrying an excess of baryons and the second—an excess of antibaryons (or vice versa, depending on the sign of $\Delta\mathcal{P}$). Moreover, the baryon asymmetry in the droplets of the QGP can get much larger than the initial lepton asymmetry once the volume fraction occupied by QGP shrinks to $\sim\mathcal{P}_0^{\frac{1}{(1+\kappa_1)}}$—an effect we will explore later in Sec. III.

The effect of matter-antimatter separation goes away if the asymmetry in reflection coefficients $\Delta\mathcal{P}_0$ is smaller than the average baryon asymmetry of the Universe. In this case, the decrease of the volume of the QGP droplets tends to increase the asymmetries in the individual quark flavors. However, these asymmetries are diluted by the weak reactions of the type $\bar{u}d \to \mu^+\nu_\mu$, $\bar{u}s \to \mu^+\nu_\mu$. As neutrinos can go easily out of the droplets, and the latter reactions are faster than the rate of the droplet shrinking $\dot{r}/r \sim H$ (H is the Hubble rate), the asymmetries in quark flavors remain at the level of the average lepton asymmetries in the Universe and do not grow with shrinking of the droplets.

Of course, the assumption that the baryon number cannot leak out of the QGP droplets is presumably too strong and is likely to be wrong at the end of the phase transition, when the density of the baryonic charge approaches that of nuclear density. The unknown strong dynamics prevented us (and the authors before, e.g., [54,70]) from making any definite conclusions concerning this point. We would like just to mention that the qualitative remark of [70] remains in force: the critical temperature of the QCD phase transition with nonzero baryon number decreases when the baryonic chemical potential increases, meaning that the QGP droplets may survive till the temperatures smaller than T_c, say $T_c/2$ [70].

The mechanism discussed above resembles a lot the scenario of domain wall electroweak baryogenesis (for a review see [83] and references therein). In the case of the first-order electroweak phase transition, the intrinsic CP-violation in interactions of quarks, leptons, or other hypothetical fermions with the domain walls also leads to the separation of fermionic number. An excess of fermions over antifermions forms inside the bubbles of a new Higgs phase, whereas the situation is opposite outside the bubbles, in the symmetric phase of the electroweak

theory. The fermionic number outside the bubbles is eaten up by equilibrium sphaleron transitions [84], which are inactive inside the bubbles if the phase transition is sufficiently strongly of the first order [85,86]. This process leads eventually to the bulk baryon asymmetry after the bubbles with symmetric phase disappear. In the QCD case the CP asymmetry is induced by the electric charge chemical potential and the sphaleron processes are not effective and thus cannot change the baryon number in either phase.

Clearly, the matter-antimatter separation scenario strongly deviates from the standard one in which the universe is homogeneous and isotropic since inflation. An obvious question is about the big bang nucleosynthesis. The sufficiently short-scale inhomogeneities disappear by the nucleosynthesis time [42–46] via the combined action of neutrino inflation and neutron diffusion.[7] Baryon number fluctuations affect BBN provided they are sizable enough over the neutron diffusion scale (3×10^5 cm) at the onset of nucleosynthesis at $T \simeq 100$ keV. The neutron diffusion scale, blue-shifted to the QCD phase transition scale $T_c \simeq 160$ MeV, becomes, $L_{\rm diff}(T_c) = 2$ m, somewhat larger than the expectation for the distance between the bubble centres, providing an estimate of the scale of baryon number fluctuations. It would be interesting to see whether this may change the BBN predictions and thus put bounds on the possible parameters of the QCD phase transition and lepton asymmetry of the Universe.

Before coming to a possible cosmological consequence of the matter-antimatter separation scenario we will consider in the next section a much more speculative possibility to have matter-antimatter separation, which would work even without the presence of (large) lepton asymmetry.

C. Omnes phase transition

Back in 1969 Omnes [87] proposed an idea of matter-antimatter separation on cosmological scales in an attempt to understand why we have only baryons in the local vicinity of our solar system. He argued that if baryons and antibaryons are repulsed from each other at small distances, the phase diagram of the strong matter allows the existence of two phases, one with an excess of baryons and another with an excess of antibaryons. If true, this would mean the spontaneous breaking of charge-conjugation symmetry in hadronic matter. According to [88,89], these phases can coexist at some interval of temperatures around ~350 MeV, and the Universe's evolution may lead to the separation of domains of matter and antimatter at the cosmological scales.

[7]The name "neutrino" inflation was introduced in [42] and has nothing to do with the cosmological inflation. It is related to the excess of pressure of the neutrinos in domains with enhanced baryonic density "inflating" these regions.

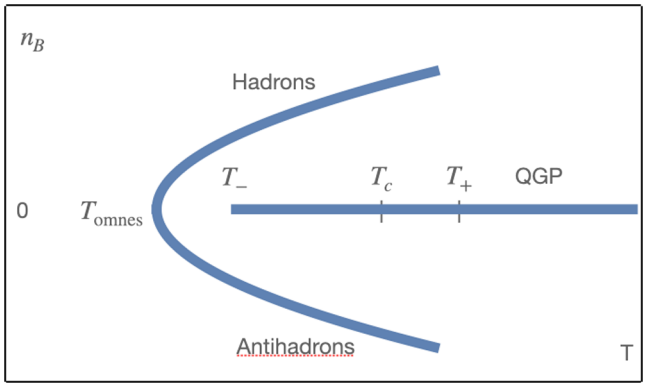

FIG. 1. Omnes type QCD phase diagram. In addition to the QGP phase with vanishing baryon number density there are two distinct hadron phases with opposite baryon number densities. The Omnes phase exists at $T_{\rm omnes} < T < T_+$, and the QGP phase at $T > T_-$.

As was noted by many researchers (see, e.g., [90,91]), the idea fails for many reasons. First, the horizon scale at temperatures ~350 MeV is too small to create any structures with masses exceeding the solar mass. Second, theoretical computations of nucleon dynamics at these temperatures cannot be reliable due to the strong coupling. Moreover, the domain of temperatures found by Omnes is already in the QGP region, where quarks and gluons provide a better description of dynamics.

Still, it seems to us that the Omnes-type phase diagram such as the one presented in Fig. 1, though extremely exotic and speculative, cannot be completely excluded. So, we find it interesting to discuss the Universe's evolution if it is indeed realized, but we cannot put any argument for why *it should be realized*.

As we have strong coupling, it would be natural to assume that at the critical temperature, the baryonic density of the Omnes states is of the order of the nuclear density, i.e., much larger than the baryon and lepton asymmetries of the Universe. In this case, the breaking of the degeneracy between the minima with different baryon numbers will be small and not essential for the initial stages of the QCD phase transition. The Omnes phase transition would start somewhat below T_c, as in the discussion in Sec. II A. However, now two types of bubbles of the hadronic phase will be nucleated. Approximately half of them will carry a positive baryon number, and another half—negative baryon number. The bubbles will grow and at some moment start to percolate, but now with the simultaneous existence of all three possible phases. The QGP phase will be eaten by the hadronic bubbles and cease to exist at temperature T_- at the latest, and we are left with domains of positive and negative baryonic number densities. The presence of lepton and baryon asymmetries, resulting in the breaking of the degeneracy, will lead to somewhat faster growth of the droplets that have lower free energy. At the temperature $T_{\rm omnes}$ (Fig. 1) the spontaneous C-breaking comes to an

end, and the Universe will be in the hadronic phase, with large inhomogeneities in the distribution of the baryon number, with a typical distance scale of the order of the initial separation between the bubble centres. At this temperature, roughly half of the space will carry a positive baryon number, and another half will be rich in antibaryons, with baryon asymmetry of the order of ± 1 in each of the domains. This is to be compared with the scenario of Sec. II B, where in the larger part of the space we have an excess of (say) matter with amplitude $\sim \Delta\mathcal{P}_0 \ll 1$, and in a smaller part of the space occupied by the QGP an excess of antimatter.

Most probably, the BBN can constrain the parameters of the Omnes-type phase transition (such as the average distance between the bubbles and the amplitude of the baryon asymmetry in different C-odd phases). This is not attempted in our paper. Instead, in the next section we will consider possible cosmological consequences of the matter-antimatter separation associated with the production of dark matter sterile neutrinos.

III. QCD PHASE TRANSITION AND PRODUCTION OF STERILE NEUTRINO DARK MATTER

A. Matter potential and resonance

For the mechanisms discussed in the literature so far, the neutrino potential in the medium was mainly determined by the lepton asymmetry of the Universe, as the baryon contribution to it is negligibly small. For the matter-antimatter separation scenarios, it is the baryon asymmetry which plays a crucial role.

The neutrino matter potential is given by [37,79] for the electron neutrino

$$V = \sqrt{2}G_F\left[2\Delta_{\nu_e} + \Delta_{\nu_\mu} + \Delta_{\nu_\tau} + \left(\frac{1}{2} + 2\sin^2\theta_W\right)\Delta_e - \left(\frac{1}{2} - 2\sin^2\theta_W\right)\Delta_\mu + \left(\frac{1}{2} - \frac{4}{3}\sin^2\theta_W\right)\Delta_u - \left(\frac{1}{2} - \frac{2}{3}\sin^2\theta_W\right)\Delta_d - \left(\frac{1}{2} - \frac{2}{3}\sin^2\theta_W\right)\Delta_s\right], \quad (3.1)$$

where Δ_i are asymmetries in the concentrations (summed over spin and color) of the corresponding fermion flavor, for instance, $\Delta_e \equiv n_e - n_{\bar{e}}$. For the temperatures of interest $T \sim 200$ MeV, the contribution of τ-lepton can be neglected. Similar expressions can be written for other types of neutrinos and also in the hadronic phase [79]. Accounting for the neutrality of the plasma expressed by Eq. (2.8), one can get from Eq. (3.1)

$$V = \frac{G_F}{3\sqrt{2}}(7L - 3B) \quad (3.2)$$

which reduces at $L \ll B$ to

$$V \approx -\frac{G_F}{\sqrt{2}}B. \quad (3.3)$$

To get a better feeling of the numbers involved, we can write the baryon number density as

$$B = \eta_B n_{h,q}, \quad (3.4)$$

where η_B is the baryon asymmetry, and n_h and n_q are the equilibrium number of baryons at zero baryon asymmetry in the hadron and QGP phases respectively. In the hadronic phase, n_h can be estimated with the use of the so-called noninteracting hadron gas approximation, counting the low-lying baryon and antibaryon states (proton, neutron, Λ-hyperon, and their excitations). At a temperature of the phase transition $T = 160$ MeV, it gives

$$n_h \simeq 0.03T^3. \quad (3.5)$$

In the QGP phase, n_q is defined in Eq. (2.11), $n_q \simeq 0.9T^3$.

Depending on the sign of V, there is a level crossing between the sterile neutrino and active neutrino or corresponding antineutrino at a certain momentum (called resonant) p, given by

$$p_{\rm res} \approx \omega_{\rm res} \approx \frac{M_1^2}{2|V|}. \quad (3.6)$$

The transition probability of neutrinos (or antineutrinos) with this momentum into sterile states is enhanced, leading to the resonant production of N. Plugging V into (3.6) we obtain expression for the resonance energy

$$\omega_{\rm res} = \frac{M_1^2}{\sqrt{2}G_F B} = \frac{M_1^2}{\sqrt{2}G_F\rho_B\eta_B}. \quad (3.7)$$

The thermal contribution to the potential [79]

$$V_T = \frac{14\pi\omega}{45}\sin^2\theta_W\frac{G_F^2T^4}{\alpha_{\rm EM}}(2 + \cos^2\theta_W), \quad (3.8)$$

can be neglected for large asymmetries considered in this work (here $\alpha_{\rm EM}$ is the fine structure constant, and θ_W is the Weinberg angle).

Let us introduce the dimensionless resonance parameter

$$x_{\rm res} \equiv \frac{\omega_{\rm res}}{T} = \frac{M_1^2}{2|V|T} = \frac{M_1^2}{\sqrt{2}G_F BT}. \quad (3.9)$$

At $T = 160$ MeV according to (3.4) and (3.5) we have in the hadronic phase

$$x_{\rm res} = \frac{0.15}{\eta_B}\left(\frac{M_1}{7\ \text{keV}}\right)^2, \quad (3.10)$$

and in the QGP phase, according to (2.11) and (3.4)

$$x_{\rm res} = \frac{0.005}{\eta_B}\left(\frac{M_1}{7\ {\rm keV}}\right)^2, \tag{3.11}$$

where the sterile neutrino mass is normalized to 7 keV having in mind the 3.5 keV line reported in several papers [33,34].

B. Resonance oscillations in infinite medium

The physics picture of $\nu - N$ transition is the following: neutrinos oscillate in between the collisions with particles of the medium. At the collisions, the coherence of the oscillating state is broken and after collisions, the active and sterile components start to oscillate independently from the beginning. Correspondingly, the relevant scales are (i) the oscillation length in medium l_m, and (ii) the mean free path: $\lambda_\nu = 1/\Gamma$.

According to this picture, the rate of production of sterile neutrinos can be written as

$$R_N(\omega) = \frac{n_F(\omega)}{(2\pi)^3} P(\omega)\Gamma, \tag{3.12}$$

where $n_F(\omega)$ is the Fermi distribution function, and $P(\omega)$ is the $\nu \to N$ oscillation probability between two collisions averaged over the distance between the collisions:

$$P(\omega) = \sin^2 2\theta_m \langle \sin^2 \phi_m \rangle. \tag{3.13}$$

The mixing angle in matter θ_m is determined by

$$\sin^2 2\theta_m = \frac{\sin^2 2\theta}{R^2_{\rm MSW}}, \tag{3.14}$$

where $R_{\rm MSW}$ is the MSW resonance factor:

$$R^2_{\rm MSW}(\omega) \equiv \cos^2 2\theta \left(1 - \frac{\omega}{\omega_{\rm res}}\right)^2 + \epsilon^2 \tag{3.15}$$

with

$$\epsilon^2 \equiv \sin^2 2\theta + \left(\frac{2\omega\Gamma}{M_1^2}\right)^2. \tag{3.16}$$

Here the last term corresponds to the broadening of the resonance due to inelastic collisions. It can be obtained by adding $-i\Gamma/2$ to the Hamiltonian of evolution, or more consistently, as the inelastic term to the equation for the density matrix.

The half-oscillation phase ϕ_m acquired along the distance x equals

$$\phi_m = \frac{\pi x}{l_m} = \frac{\pi x R_{\rm MSW}(\omega)}{l_\nu}, \tag{3.17}$$

and the oscillation length in a medium is

$$l_m = \frac{l_\nu}{R_{\rm MSW}(\omega)} = \frac{4\pi\omega}{M_1^2 R_{\rm MSW}(\omega)}. \tag{3.18}$$

Inserting expression for probability into (3.12) we obtain the rate of N-production

$$R_N = \frac{n_F(\omega)}{(2\pi)^3}\Gamma \frac{1}{R_{\rm MSW}(\omega)^2}\langle \sin^2\phi_m \rangle. \tag{3.19}$$

The quantity ϵ (3.16) can be rewritten as

$$\epsilon^2 = \sin^2 2\theta \left[\left(\frac{l_R}{2\pi\lambda_\nu}\right)^2 + 1\right], \tag{3.20}$$

where $l_R = l_\nu/2\theta$ is the oscillation length in resonance (in the absence of collisions), $l_R \gg l_\nu, l_0$. In the epoch of the QCD phase transition $\lambda_\nu \ll l_R/2\pi$ and the second term in (3.20) can be neglected. Then the expression for the rate of N-production (3.19) becomes explicitly (taking $c_{2\theta} = 1$)

$$R_N = \frac{n_F}{(2\pi)^3} 4\theta^2 M_1^4 \frac{\Gamma}{(M_1^2 - 2\omega V)^2 + (2\omega\Gamma)^2}\langle \sin^2\phi_m \rangle. \tag{3.21}$$

The key feature of these oscillations is that due to the smallness of vacuum mixing the oscillation length in matter changes with E by many orders of magnitude: in resonance $l_m = l_R = l_\nu/\sin 2\theta \approx l_\nu/2\theta$, while below resonance $l_m \approx l_\nu$, and above resonance $l_m \approx l_0$, $l_R \gg l_\nu$. So, $l_m \gg \lambda_\nu$ in resonance, while $l_m \ll \lambda_\nu$ outside the resonance. This means that outside the resonance the oscillations between two collisions are averaged, and consequently $\sin^2\phi_m = 1/2$. The resonance peak exists but its width and height are determined by collisions. The oscillation phase between two collisions equals

$$\phi_m = \pi\frac{\lambda}{l_m} \approx \frac{\lambda}{2}\sqrt{\left(\frac{M_1^2}{2\omega} - V\right)^2 + \Gamma^2} \tag{3.22}$$

and in the resonance $\phi_m \approx \lambda\Gamma/2 \approx 1/2$.

Here we computed the rate of production of N by a single active neutrino. If we neglect the term $(M_1^2 \sin 2\theta)^2$ and assume for simplicity the same potential V for all neutrino species (which is justified if the neutral current scattering on quarks dominates), then summation over active neutrinos is reduced to considering θ^2 as the overall vacuum mixing angle squared:

$$\theta^2 \equiv \sum \theta_\alpha^2.$$

Using relation

$$\frac{\alpha}{(x_{\rm res} - x)^2 + \alpha^2} = \pi\delta(x - x_{\rm res}) + O(\alpha), \tag{3.23}$$

we can rewrite the rate (3.21) as

$$R_N \approx \frac{n_F}{(2\pi)^2}\frac{\theta^2 M_1^4}{2\omega V}\delta(\omega-\omega_{\rm res})\langle\sin^2\phi_m\rangle = \frac{n_F}{(2\pi)^2}\theta^2 M_1^2\langle\sin^2\phi_m\rangle\delta(\omega-\omega_{\rm res}), \quad (3.24)$$

where we used (3.6). For $\sin^2\phi_m = 1/2$ it coincides with the expression obtained from the first principle computation of the resonance contribution in [36]

$$R_N = \frac{n_F(\omega)}{(2\pi)^2 2\omega}\theta^2 M_1^4\delta(M_1^2 - 2\omega V). \quad (3.25)$$

This result is valid in the narrow width approximation, $\Gamma_{\nu_e} \ll |V|$.

For very high interaction rate: $\Gamma \gg 2\pi/l_0 \gg 2\pi/l_R$, (wide width) the resonance peak essentially disappears and we cannot use the δ- function approximation (3.23). Formally the oscillation length becomes $l_m \approx 2\pi/\Gamma$ and the oscillation phase acquired between two collisions is $\phi_m = 1/2$. The rate of N-production equals according to (3.24)

$$R_N = \frac{n_F}{(2\pi)^3}\frac{\theta^2 M_1^4}{\omega^2\Gamma}\langle\sin^2\phi_m\rangle \quad (3.26)$$

with $\sin^2\phi_m \leq 1/4$. In the opposite extreme case of very low interaction rate, $\lambda_\nu \gg l_R/2\pi$, the vacuum term $(M_1^2 s_{2\theta})^2$ in the denominator of (3.19) dominates and we obtain

$$R_N = \frac{n_F}{(2\pi)^2}\frac{\Gamma\theta^2 M_1^2}{4V}\delta(\omega-\omega_{\rm res}) = \frac{n_F}{(2\pi)^2}\frac{\Gamma\theta^2\omega_{\rm res}}{2}\delta(\omega-\omega_{\rm res}). \quad (3.27)$$

Thus, the rate of N production has the following dependence on Γ: for low Γ, $R_N \propto \Gamma$, in the intermediate range the rate does not depend on Γ and for large Γ, $R_N \propto 1/\Gamma$.

To get the total number density of sterile neutrinos, n_N, the rate R_N in Eq. (3.24) should be integrated over time and momentum

$$n_N = \int dt\int d^3p R_N(\omega) = 4\pi\int dt\int d\omega\omega^2 R_N(\omega). \quad (3.28)$$

Integration over energy is trivial due to the δ- function, giving

$$n_N = \frac{1}{2\pi}\theta^2 M_1^2\int dt n_F(\omega_{\rm res})\omega_{\rm res}^2\langle 2\sin^2\phi_m\rangle. \quad (3.29)$$

For $\langle 2\sin^2\phi_m\rangle = 1$ the concentration of resonantly produced sterile neutrinos at the time t is given by

$$n_N(t) = \frac{1}{2\pi}\theta^2 M_1^2 T(t)^3\int_0^t\frac{dt'}{T(t')}n_F(x_{\rm res})x_{\rm res}^2, \quad (3.30)$$

which is the same as Eq. (2.7) of [36], rewritten in terms of time integral rather than the temperature one.

Assuming that the production of the sterile neutrinos stops at temperature T corresponding to t, their concentration at the present epoch can be found with the use of the entropy conservation by a standard computation, giving

$$n_N(\text{now}) = n_N(t)\frac{s(\text{now})}{s(T)}, \quad (3.31)$$

where $s(\text{now})/s(T) = g^*(\text{now})/g^*(T)(T_\gamma/T)^3$ with $g^*(\text{now}) = 3.9$, and $T_\gamma = 2.73\,\text{K}$ being the temperature of the CMB. Thus the ratio of energy density in sterile neutrinos to DM energy density is given by

$$\frac{\Omega_N}{\Omega_{\rm DM}} = \frac{n_N M_1}{\Omega_{\rm DM}}\frac{s(\text{now})}{s(T)}. \quad (3.32)$$

For a future comparison, we present below an estimate of the sterile neutrino DM abundance in the homogeneous situation in the presence of both baryon and lepton asymmetries, see Eq. (3.2). In the assumption of standard cosmology without the QCD phase transition and neglecting the temperature dependence of g^* the integral in (3.30) can be computed analytically, giving the abundance of the resonantly produced sterile neutrino,

$$\frac{\Omega_N}{\Omega_{\rm DM}} \simeq 10^{16}\theta^2\left[\frac{1}{g^*}\left|\Delta_L - \frac{3}{7}\Delta_B\right|\left(\frac{M_1}{7\text{ keV}}\right)^2\right]^{3/4}. \quad (3.33)$$

The temperature of the maximal production rate equals

$$T_{\rm prod} \simeq 380\text{ MeV}\left(\frac{M_1}{7\text{ keV}}\right)^{\frac{1}{2}}\left[\frac{1}{g^*(T)}\frac{6.6\times10^{-5}}{\Delta_L}\right]^{\frac{1}{4}}, \quad (3.34)$$

where we used the observed DM abundance $\Omega_{\rm DM} = 1.26\times10^{-6}\ \text{GeV/cm}^{-3}$. The formula (3.33) overestimates the number of sterile neutrinos by a factor of a few. It does not take into account the thermal contribution (3.8) to the matter potential, which cuts the resonance at high temperatures. Also, the delta-function approximation to the rate (3.27) becomes invalid at temperatures large enough, where the resonance is suppressed by the active neutrino collisions. Finally, it does not incorporate the depletion of lepton asymmetry because of the resonance transitions of active to sterile neutrinos and temperature dependence of g^*.

The most elaborated analysis of the sterile neutrino production in lepton asymmetric homogeneous Universe, accounting for the finite width of the neutrino, the back reaction of produced sterile neutrinos, and nonresonant production can be found in [37].

With these considerations, we are now in a position to estimate the sterile neutrino production in matter-antimatter separating QCD phase transition. We will discuss first a simpler, but more exotic possibility of the Omnes phase transition (Sec. II C). Then we will turn to a more realistic scenario of Sec. II B.

C. Sterile neutrino DM production with matter-antimatter domains

Suppose that the Universe is filled by matter-antimatter domains at the QCD epoch. This may happen due to hypermagnetic fields [47–49], inhomogeneous baryogenesis [50–52], or Omnes-type QCD phase transition, discussed in Sec. II C. The origin of these domain is not essential in what follows, though for concreteness we chose it to be the (speculative) Omnes-type phase transition.

As we discussed in Sec. II C, at temperatures below T_-, half of the universe is occupied by hadronic matter with the baryon excess, and another part contains an excess of antimatter. In both parts, the resonant production of sterile neutrinos takes place by neutrinos and antineutrinos. Contrary to the homogeneous situations, the sterile neutrinos will be produced in left- or right-handed polarizations, depending on the sign of the baryon asymmetry in a given domain.[8] So, production here is essentially the same as in a homogeneous background.

If characteristics of medium n, T do not change substantially during phase transition, then according to (3.30) the total number density of N produced during the time $t_{\rm PT}$ is

$$n_N \approx \frac{n_F(x_{\rm res})}{2\pi}\theta^2 M_1^2 x_{\rm res}^2 T_{\rm PT}^2 t_{\rm PT}. \tag{3.35}$$

We expect that this equation gives a fairly good account of the sterile neutrino production, but in reality, one would need to take into account the change of parameters of the medium during the phase transition (and even after the matter-antimatter domain structure existed). This is not attempted here because of the many uncertainties involved. It is clear that only an order of magnitude estimate can be made at the present stage, as even the mere existence of the Omnes-type phase transition is speculation. We note, however, that contrary to Eq. (3.33) the depletion of the lepton asymmetry due to resonant transition can indeed be neglected since the matter potential is due to baryon rather than lepton asymmetry. Also, the temperature at which the process of conversion happens is relatively small, justifying the delta-function approximation of the rate and dropping off the thermal contribution to the potential.

[8]Anyway, the polarization of sterile neutrinos is "forgotten" in the course of further evolution of the Universe due to their interaction with the gravitational field of galaxies and clusters of galaxies [92].

Equation (3.35) leads to the sterile neutrino DM abundance

$$\frac{\Omega_N}{\Omega_{\rm DM}} \simeq 4\times 10^{12}\theta^2\left(\frac{M_1}{7\ {\rm keV}}\right)^3 x_{\rm res}^2 n_F(x_{\rm res})\frac{t_{\rm PT}}{t_H}. \tag{3.36}$$

This formula shows that the matter-antimatter separating Omnes phase transition can easily accommodate 100% sterile neutrino DM abundance for ranges of mixing angles and masses. For example, keeping in mind the possible detection of 7 keV sterile neutrino decays by x-ray satellites [33,34] with $\theta^2 \simeq (0.8\text{–}5)\times 10^{-11}$, the choice $\theta = 1.5\times 10^{-11}$, $t_{\rm PT} \simeq t_H/4$, and $\eta_B \simeq 1/2$ does the job. An interesting feature of the sterile DM distribution is that it can be much cooler than that of the typical active neutrino with $\langle\omega\rangle \simeq 3.15T$. Indeed, according to (3.10) $\omega_{\rm res}/\langle\omega\rangle = x_{\rm res}/3.14 \simeq 0.1$ for $\eta_B \simeq 1/2$, making it essentially the cold dark matter particle, which satisfies easily all the Lyman-α [35] and the strongest structure formation constraints of [93–96].

D. Sterile neutrino production in nonuniform medium with large QGP droplets

Let us assume now that the QCD phase transition goes as described in Sec. II B via the formation of QGP droplets with enhanced baryon number. Also, we take that the average value of the leptonic asymmetry is much larger than the baryon asymmetry but smaller than the critical value $L_{\rm crit} \simeq 6.6\times 10^{-5}$. In this case, 7 keV sterile neutrinos with the mixing angle $\theta^2 = 5\times 10^{-11}$ cannot accommodate all DM in the Universe if the QCD phase transition were absent.

The key feature of this scenario is that the droplets of QGP shrink, and consequently, the baryon number density in them increases. That is, soon after the time of formation of droplets t_0 (percolation time of hadron bubbles), the baryon number density inside the droplets, n_B^d, grows like in Eq. (2.13), with omitted first term. The last term in the bracket gives

$$n_B^d(t) = n_B^d(t_0)\left[\frac{r(t_0)}{r(t)}\right]^3, \qquad n_B^d(t_0) = \Delta\mathcal{P}_0 n_q. \tag{3.37}$$

For later times, the baryon density would follow (2.16).

Depending on the initial size of the QGP droplets at the percolation t_0, computations of the sterile neutrino yield proceed in two different ways.

If the initial droplet sizes r_d are much larger the neutrino mean free path λ_ν (say $r_0 \sim 1$ m while $\lambda_\nu \sim 0.4$ cm (see Sec. II B)), the processes of sterile neutrino production described in the previous subsection take place inside the droplet. We will assume that the baryon number density inside the droplets does not depend on distance and surface effects are negligible. Also, we will neglect oscillations between the droplets, since the baryon and lepton

asymmetries there are assumed to be below the critical value. Thus, these domains cannot produce enough sterile neutrino DM.

To get the number of sterile neutrinos produced inside the droplets, one can repeat the procedure leading to (3.30), but accounting for the fact that only the part of space occupied by the droplets, $V_{\rm QGP}$, leads to N- creation. Furthermore, this part decreases with time. The total volume can be presented as $V_{\rm tot} = V_{\rm QGP} + V_{\rm h} \approx 2V_{\rm QGP}(t_0)$, that is, in the initial moment about half of the space is occupied by droplets. Then the QGP part as a function of time equals

$$\frac{V_{\rm QGP}(t)}{V_{\rm tot}} = \frac{V_{\rm QGP}(t)}{2V_{\rm QGP}(t_0)} \equiv \frac{1}{2}F(t), \tag{3.38}$$

and consequently, according to (3.30)

$$n_N(t) = \frac{\theta^2 M_1^2 T^2}{4\pi}\int_{t_1}^{t} dt x_{\rm res}^2 n_F(x_{\rm res}) F(t), \tag{3.39}$$

where we neglected the sterile neutrino production between t_0 and t_1.

Now the resonance energy depends on the baryon number density in the droplets and therefore on time due to droplet contraction. Indeed, we have

$$x_{\rm res}(t) = x_{\rm res}(t_1)\frac{n_B^d(t_1)}{n_B^d(t)} = x_{\rm res}(t_1)F(t)^{1+\kappa_1}, \tag{3.40}$$

where the initial value of the resonance parameter can be taken at time t_1 defined below Eq. (2.14) and κ_1 in (2.15), and is equal to

$$x_{\rm res}(t_1) = \frac{M_1^2}{\sqrt{2}G_F n_B^d(t_1) T} = \frac{M_1^2}{\sqrt{2}G_F n_q \Delta\mathcal{P}_0 T}. \tag{3.41}$$

Here the total density of hadrons n_q is defined in (2.11) while the difference of reflection coefficients $\Delta\mathcal{P}_0 \propto \kappa$— in (2.9) and (2.15).

Thus, the number of created sterile neutrinos depends in an essential way on the evolution of the fraction of the QGP, which is largely unknown. The ratio $\frac{\Omega_N}{\Omega_{\rm DM}}$ is given by (3.32) where n_N is to be taken from (3.39) and $x_{\rm res}(t_1)$ from (3.41).

A very rough estimate can be derived with a function $F(t)$ which starts at 1 at $t = t_1$, quickly decreases to a constant F_0, and then at the end of the phase transition falls to $F(t) = 0$, reproducing the initial growth of the baryon density, then slowing down the droplet shrinking because of the extra pressure acting from inside, and finally the droplet disappearance. For numeric computations below we use $F(t) = F_0$ in the range $t_0 - t_f$. The dependence of the sterile neutrino DM abundance defined in (3.39) on F_0 then is given by

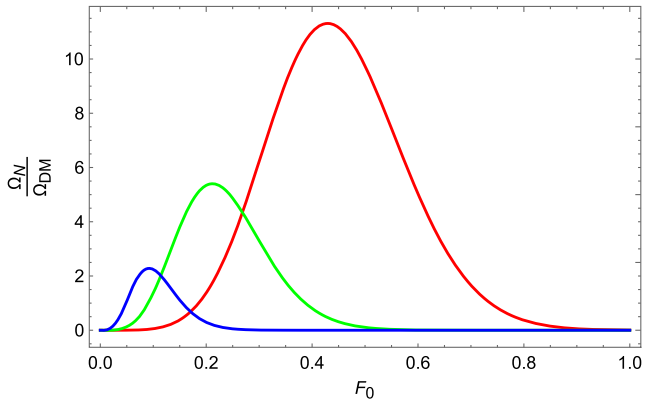

FIG. 2. Dependence of the ratio $\frac{\Omega_N}{\Omega_{\rm DM}}$ (vertical axis) on F_0 (horizontal axis) for $M_1 = 7\,\text{keV}$, $\theta^2 = 5\times10^{-11}$, and $\Delta_L = L_{\rm crit}$. Red, green and blue curves correspond to $\kappa = \kappa_1 = 1, 1/2$ and $1/4$ respectively.

$$n_N = \frac{\theta^2 M_1^2 T^2}{4\pi}\frac{F_0^{3+2\kappa_1} x_{\rm res}^2(t_1) t_{\rm PT}}{\exp[x_{\rm res}(t_1)F_0^{1+\kappa_1}] + 1}. \tag{3.42}$$

The ratio $\Omega_N/\Omega_{\rm DM}$ determined by n_N according to (3.32) is shown in Fig. 2. It demonstrates that n_N can exceed the required DM abundance for $\Delta_L = L_{\rm crit}$ for a wide range of parameters characterizing the unknown dynamics of the droplet shrinking. In other words, the QCD phase transition may enhance the sterile neutrino production and lead to 100% of its abundance even if the lepton asymmetry is smaller than the critical one, though to see if this indeed happens would require the precise knowledge of the droplet dynamics. As follows from Fig. 2, in the wide ranges of values of κ_1 and F_0, one has $\Omega_N/\Omega_{\rm DM} \gg 1$, which means that $\Omega_N = \Omega_{\rm DM}$ can be obtained for much smaller lepton asymmetry than $L_{\rm crit}$.

To get a feeling of how small the required asymmetry could be, we present in Fig. 3 the dependence of the sterile neutrino abundance following from Eq. (3.42) on F_0 for different values of the ratio $\Delta_L/L_{\rm crit}$, κ and κ_1, which are chosen in such a way that the maxima of the corresponding curves reach one at some value of F_0. Even the asymmetries smaller than the critical one by a factor of 100 are possible for the specific choice of $F_0 \simeq 0.04$.

A somewhat more involved time dependence of the QFP fraction can be written as

$$F(t) = \left(\frac{t_f - t}{t_{\rm PT}}\right)^{\alpha}, \tag{3.43}$$

where t is time, t_f (t_i) corresponds to the end (beginning) of the phase transition so that $t_{\rm PT} \equiv t_f - t_i$. We leave the power α to vary between 1 and 3: $\alpha = 1$ corresponds to the behavior found in [54] by solving FRW equations during the QCD phase transition assuming the entropy conservation, whereas $\alpha = 3$ would correspond to the motion of the

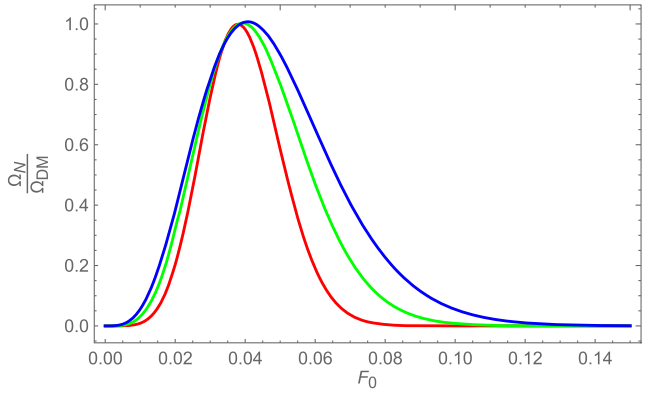

FIG. 3. Dependence of the ratio $\frac{\Omega_N}{\Omega_{\rm DM}}$ (vertical axis) on F_0 (horizontal axis) for $M_1 = 7$ keV, $\theta^2 = 5 \times 10^{-11}$ for different values of the ratio $\Delta_L/L_{\rm crit}$ and κ, κ_1. Red, green, and blue curves correspond to $\kappa = \kappa_1 = 1$; $\Delta_L/L_{\rm crit} = 0.008$, $\kappa = \kappa_1 = 1/2$; $\Delta_L/L_{\rm crit} = 0.08$, and $\kappa = \kappa_1 = 1/4$; $\Delta_L/L_{\rm crit} = 0.4$ respectively.

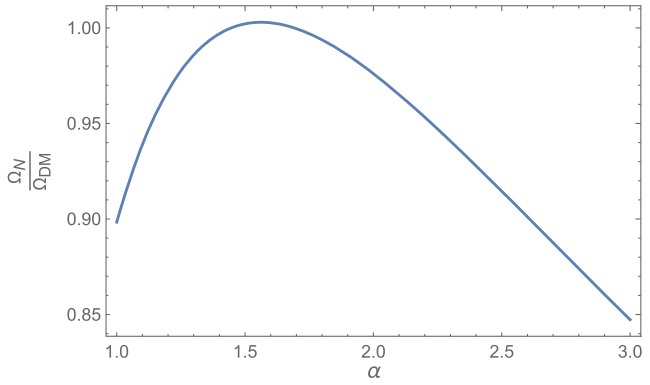

FIG. 4. Dependence of the ratio $\frac{\Omega_N}{\Omega_{\rm DM}}$ (vertical axis) on α (horizontal axis) for $M_1 = 7$ keV, $\theta^2 = 5 \times 10^{-11}$, and $\Delta_L = L_{\rm crit}/4$.

bubble walls with the constant velocity, accounting for friction, often found in electroweak baryogenesis (see, e.g., [97]). It is difficult to argue that the QGP fraction is indeed described by (3.43) because of poor knowledge of the dynamics of the phase transition.

After straightforward manipulations with Eqs. (3.38) and (3.43) we get

$$n_N = \frac{\theta^2 M_1^2 T^2}{8\pi}\left[\frac{\sqrt{2} G_F T \Delta \mathcal{P} n_q}{M_1^2}\right]^{\frac{\alpha+1}{\alpha(1+\kappa_1)}} I(\alpha) t_{\rm PT}, \tag{3.44}$$

where the integral I is given by

$$I = \frac{1}{(1+\kappa_1)\alpha}\int_{x_{\rm res}(t_f)}^{x_{\rm res}(t_i)} dx_{\rm res} x_{\rm res}^{1+\frac{\alpha+1}{\alpha(1+\kappa_1)}} n_F(x_{\rm res}). \tag{3.45}$$

The limits of integration can be safely extended from zero to infinity. Indeed, since we take $\Delta_L < L_{\rm crit}$, the upper limit in (3.45) exceeds considerably 1, and at the end of the phase transition the baryon asymmetry inside the droplet formally diverges, making $x_{\rm res}(t_f) = 0$.

In Fig. 4 we show the sterile neutrino DM abundance following from Eq. (3.44) as a function of α for $\Delta_L = L_{\rm crit}/4$, demonstrating that certain droplet dynamics can generate enough sterile neutrinos for asymmetries smaller than the critical one, in this case for $\alpha \simeq 1.5$.

E. Oscillations in medium with small droplets

Let us consider now the situation in which the initial size of the droplets is smaller than the neutrino mean free path λ_ν. Since $\lambda_\nu \propto 1/n_{\rm tot}$ and inside the droplets total number density $n_{\rm tot}$ may only weakly increase the inequality $r_d < \lambda_\nu$ will maintain during phase transition. In this case, a given active neutrino can cross two or more droplets.

Now we have the following relation between the scales

$$l_\nu \sim l_0 \ll r_d \ll l_\nu^R, \tag{3.46}$$

where r_d is the radius of the droplet. If the droplets have a spherical form the average distance crossed by neutrinos is $\bar{r} = (\pi/2) r_d$. At the conditions (3.46) the oscillation phase in the MSW resonance: $\phi_R(\bar{r}) \ll 1$, while in the tails above and below resonance energy $\phi \gg 1$. Therefore the probability of the $\nu \to N$ conversion in the energy range close to the resonance energy $E \simeq E_{\rm res}$ is given by

$$P \approx \sin^2\theta \left(\frac{\pi \bar{r}}{l_\nu}\right)^2, \tag{3.47}$$

$R_{\rm MSW}$ cancels and the probability does not depend on the matter density (the so-called "vacuum mimicking" regime [98,99]). Exactly at $\omega = \omega_{\rm res}$

$$P_{\rm res} \approx 4\pi^2\theta^2\left[\frac{\bar{r}}{l_\nu(\omega_{\rm res})}\right]^2. \tag{3.48}$$

The probability as a function of energy has a peak inscribed into the MSW resonance peak with maximal value $\approx P_{\rm res}$ (3.48). The width of the peak, $\delta\omega = \omega_W - \omega_{\rm res}$, is determined approximately by the condition that the oscillation phase in matter equals $\pi/2$:

$$\phi_m(\omega_W) = \frac{\bar{r} M_1^2 R_{\rm MSW}(\omega_W)}{4\omega_W} = \frac{\pi}{2}. \tag{3.49}$$

The solution of equation (3.49) is

$$\frac{\delta\omega}{\omega} \equiv \left(1 - \frac{\omega_W}{\omega_{\rm res}}\right) \approx \pm \frac{l_\nu(\omega_{\rm res})}{\bar{r}} \approx \left(\frac{l_\nu}{2\bar{r}}\right). \tag{3.50}$$

At ω_W the peak touches the MSW resonance line. The probabily is zero at $\phi_m = \pi$, i.e. at $\delta\omega/\omega = l_\nu/r_d$. At the

points $\omega = \omega_W$, the probability equals $P_W = 16\theta^2(\bar{r}/l_\nu)^2$. Consequently, $P_{\rm res}/P_W = \pi^2/4 = 2.46$, that is, $\delta\omega/\omega$ is the width at approximately half of the height of the peak. Notice that in contrast to the case of big droplets here the biggest energy scale $1/\bar{r}$ plays the role of Γ and determines the properties of the peak.

The $\nu \to N$ oscillation probability averaged over the spectrum of active neutrinos equals

$$\langle P_N \rangle = \frac{1}{n_\nu} 4\pi \int d\omega \omega^2 \frac{n_F(\omega)}{(2\pi)^3} P_N(\omega) \approx P_{\rm res} z(2\delta\omega), \tag{3.51}$$

where $n_\nu = 3\zeta(3)/(4\pi^2)T^3$ is the neutrino concentration (one chiral degree of freedom) and

$$z(2\delta\omega) = \frac{1}{n_\nu} 4\pi \int_{2\delta\omega} d\omega \omega^2 n_F(\omega) = \frac{4}{3\zeta(3)} \left(\frac{\omega_{\rm res}}{T}\right)^3 n_F(\omega) \frac{\delta\omega}{\omega} \tag{3.52}$$

is the fraction of active neutrinos in the energy interval $2\delta\omega$. Here we have taken into account the contribution of the peak of $P(\omega)$ to the integral. The contribution of the nonresonance tails can be estimated using the averaged oscillation probability in a vacuum taking $\delta\omega/\omega \sim 1$. This gives $\langle P_N \rangle \sim 2\theta^2$, smaller than resonance contribution by a factor $2\pi^2\bar{r}/l_\nu \gg 1$ and can be neglected. Inserting the fraction (3.52) into (3.51) we obtain

$$\langle P_N \rangle \approx \frac{2\pi}{3\zeta(3)} \frac{\theta^2 M_1^2 \bar{r}}{T} \left(\frac{\omega_{\rm res}}{T}\right)^2 n_F(\omega_{\rm res}). \tag{3.53}$$

This is averaged over the energy probability that the active neutrino produces a sterile neutrino while crossing a droplet.

Using $\langle P_N \rangle$ the total production rate of sterile neutrino number density R_N can be obtained in two different ways.

1. Consider a given active neutrino propagating in a medium with QGP droplets with number density n_{drop}. The rate of N- production equals

$$R_N = \langle P_N \rangle P_{\rm drop} n_\nu, \tag{3.54}$$

where $P_{\rm drop}$ is the probability that active neutrino hits the droplet in the unit of time

$$P_{\rm drop} = \sigma_{\rm drop} n_{\rm drop}. \tag{3.55}$$

Here $\sigma_{\rm drop} = \pi r_d^2(t)$ is the area (cross section) of the droplet. Inserting all the factors into (3.54) gives

$$R_N = \langle P_N \rangle \pi r_d^2(t) n_{\rm drop} n_\nu. \tag{3.56}$$

This computation is similar to the computation of the process of scattering $\nu +$ droplet $\to N +$ droplet.

2. Consider a given droplet and compute the number of sterile neutrinos produced in this droplet in the unit of time

$$n_N = \langle P_N \rangle F_\nu n_{\rm drop}, \tag{3.57}$$

where F_ν is the active neutrino flux entering the droplet: $F_\nu = 0.5 n_\nu S_{\rm drop} = 2\pi r_d^2(t) n_\nu$. Here $S_{\rm drop}$ is the surface of a droplet and factor 0.5 accounts that only half of neutrinos in a given point of the surface enter a droplet. Collecting all the factors we obtain from (3.57)

$$n_N = \langle P_N \rangle 2\pi r_d^2(t) n_\nu n_{\rm drop}, \tag{3.58}$$

which coincides with expression (3.56).

The number density of droplets $n_{\rm drop} = 1/d^3$. Here d is the distance between the centers of droplets. It does not change with time, while the radius of the droplet decreases with time $d \approx 2r_d(t_0)$, where $r_d(t_0)$ is the initial radius of the droplet. Inserting expression for $n_{\rm drop}$ into (3.56) and integrating over time we obtain

$$n_N = \pi n_\nu \int dt \langle P_N \rangle r_d^2(t) \frac{1}{(2r_d(t_0))^3}. \tag{3.59}$$

Then using explicit expression for $\langle P_N \rangle$ from (3.53) we find

$$n_N = \frac{\theta^2 M_1^2}{16} \int dt \omega^2 n_F(\omega) \left(\frac{r_d(t)}{r_d(t_0)}\right)^3. \tag{3.60}$$

This result coincides up to a factor of the order one with expression for n_N in the case of large droplets (3.39) (16 in the denominator should be substituted by 4π), which is not accidental. Consequently, further integration over t proceeds in the same way as in the Sec. III D. Therefore, the oscillations of active neutrinos in the small droplets of QGP with large baryon density may also lead to enhanced sterile neutrino production.

As previously, the required lepton asymmetry to accommodate the totality of DM may be considerably smaller (say, a factor of 10 or even 100, as we saw in the previous section) than the critical one, though a reliable estimate of the lower bound on Δ_L is hardly possible with the current uncertainties. In comparison with the resonant production in the homogeneous universe (3.33), the gain is explained by the interplay of different factors, such as an increased neutrino potential in the droplets of the QGP at the QCD phase transition, and distinct time evolution of the neutrino potential. As a result, the parametric dependences of the abundance on the mass of the sterile neutrino and asymmetry in both cases are different.

IV. DISCUSSION AND OUTLOOK

In this paper, we considered the production of DM sterile neutrinos in an inhomogeneous Universe, temporarily filled by matter-antimatter domains at temperatures of the order of the QCD scale. For this, we assumed that the QCD phase transition is of the first order. Recent NANOGrav results on stochastic gravitational waves give some hint in favor of such a possibility.

We argued that the QCD phase transition may lead to matter-antimatter separation. This is a speculation about the complicated strong dynamics: the existence of the phase transition is a strong assumption, whereas neither the existence of the Omnes-type phase transition nor the CP-breaking properties of the interphase tension between the hadronic phase and the QGP in the presence of lepton asymmetries were derived from the first principles and are simply assumed.

The most robust part of our work is associated with sterile neutrino DM production in the nonhomogeneous situation. The consideration includes several parameters of the phase transition and bubble evolution such as the initial size of the bubbles, the exponent α, etc. The values of these parameters should follow from a quantitative description of the dynamics of the transitions which is not known yet. Therefore we assumed certain intervals for these parameters and considered different cases. We have found however that final results depend on these uncertainties weakly. If the matter-antimatter separation takes place by the considered here or some other mechanisms (for instance, due to the possible existence of stochastic hypermagnetic fields [47]), the production of sterile neutrino dark matter may be enhanced in comparison with the homogeneous situation. For the very speculative Omnes-type phase transition, we found that one can easily accommodate all DM in sterile neutrinos. In another, more realistic scenario (with two coexisting phases and a CP-violating boundary due to the presence of lepton asymmetry) the DM sterile neutrinos may be effectively produced even if the lepton asymmetry is ∼4–5 orders of magnitude larger the average baryon asymmetry in the Universe $\Delta_L \sim 10^{-6}$, that is two orders of magnitude smaller than the critical value for uniform medium.

Let us underline that the lepton asymmetry plays in the standard scenario of uniform medium and in our case different role. In the usual case, this asymmetry determined immediately the matter potential $V \propto L$ which leads to the resonance production of sterile neutrinos. In our case, the potential is given by baryon asymmetries in the bubbles. The lepton asymmetry is needed for matter-antimatter separation on the bubble walls between two phases.

The result on smaller required lepton asymmetry may shed light on the mass scale of the heavier HNL's in the νMSM. If the distribution of the lepton number is homogeneous, the asymmetry $L_{\rm crit}$, necessary for the sterile neutrino DM production can be generated in out-of-equilibrium decays of $N_{2,3}$ [38–40]. This requires, however, a delicate fine-tuning between the Majorana mass splitting and the Higgs-induced HNL mass splitting due to mixing with active neutrinos [100], to make the physical mass difference between $N_{2,3}$ small and enhance the CP-violating effects. If this fine-tuning, which may not seem to be natural, is absent, the νMSM interactions are not capable of generating asymmetries as large as $L_{\rm crit}$ [75]. However, the production of asymmetries $\Delta_L \sim 10^{-6}$ is possible at the freeze-out of the HNL's *without the above-mentioned fine-tuning* in the limited domain of the HNL masses. Indeed, Figs. 8 and 9 of [75] show that the asymmetry, $\Delta_L \gtrsim 10^{-5}$ can be generated in the νMSM only for HNL masses in the interval [1–2.5] GeV if the neutrino mass ordering is normal and no viable interval exists for the inverted ordering. The asymmetry larger than $\Delta_L \sim 10^{-6}$ can be generated for somewhat larger intervals of HNL masses: [0.2–4.5] GeV for normal ordering and [0.2–1.5] GeV for inverted one. This may serve as the very first indication of the scale of the mass of HNLs: the explanation of neutrino masses and baryogenesis, together with BBN constraints only provides a lower bound on their mass, $M_N >$ 140 MeV (for a review see [101]). Generation of the sterile neutrino Dark matter without mass fine-tuning puts the upper bound at 4–5 GeV. The search for HNL's in this mass domain is potentially possible at the intensity frontier of particle physics, in the experiments like SHiP at CERN SPS [102].

ACKNOWLEDGMENTS

The work of M. S. was supported by the Generalitat Valenciana Grant No. PROMETEO/2021/083. M. S. also thanks Harvey Meyer for the discussion of the lattice simulations of the QCD phase transition.

[1] S. Dodelson and L. M. Widrow, Sterile-neutrinos as dark matter, Phys. Rev. Lett. **72**, 17 (1994).

[2] X.-D. Shi and G. M. Fuller, A new dark matter candidate: Nonthermal sterile neutrinos, Phys. Rev. Lett. **82**, 2832 (1999).

[3] B. T. Cleveland, T. Daily, R. Davis, Jr., J. R. Distel, K. Lande, C. K. Lee, P. S. Wildenhain, and J. Ullman, Measurement of the solar electron neutrino flux with the Homestake chlorine detector, Astrophys. J. **496**, 505 (1998).

[4] J. N. Abdurashitov *et al.* (SAGE Collaboration), Measurement of the solar neutrino capture rate with gallium metal, Phys. Rev. C **60**, 055801 (1999).

[5] J. N. Abdurashitov *et al.* (SAGE Collaboration), Solar neutrino flux measurements by the Soviet-American Gallium Experiment (SAGE) for half the 22 year solar cycle, J. Exp. Theor. Phys. **95**, 181 (2002).

[6] W. Hampel *et al.* (GALLEX Collaboration), GALLEX solar neutrino observations: Results for GALLEX IV, Phys. Lett. B **447**, 127 (1999).

[7] M. Altmann *et al.* (GNO Collaboration), GNO solar neutrino observations: Results for GNO I, Phys. Lett. B **490**, 16 (2000).

[8] S. Fukuda *et al.* (Super-Kamiokande Collaboration), Solar ^8B and HEP neutrino measurements from 1258 days of Super-Kamiokande data, Phys. Rev. Lett. **86**, 5651 (2001).

[9] Q. R. Ahmad *et al.* (SNO Collaboration), Measurement of the rate of $\nu_e + d \to p + p + e^-$ interactions produced by ^{8}B solar neutrinos at the Sudbury Neutrino Observatory, Phys. Rev. Lett. **87**, 071301 (2001).

[10] Q. R. Ahmad *et al.* (SNO Collaboration), Direct evidence for neutrino flavor transformation from neutral current interactions in the Sudbury Neutrino Observatory, Phys. Rev. Lett. **89**, 011301 (2002).

[11] K. Eguchi *et al.* (KamLAND Collaboration), First results from KamLAND: Evidence for reactor anti-neutrino disappearance, Phys. Rev. Lett. **90**, 021802 (2003).

[12] T. Araki *et al.* (KamLAND Collaboration), Measurement of neutrino oscillation with KamLAND: Evidence of spectral distortion, Phys. Rev. Lett. **94**, 081801 (2005).

[13] Y. Fukuda *et al.* (Super-Kamiokande Collaboration), Evidence for oscillation of atmospheric neutrinos, Phys. Rev. Lett. **81**, 1562 (1998).

[14] Y. Ashie *et al.* (Super-Kamiokande Collaboration), Evidence for an oscillatory signature in atmospheric neutrino oscillation, Phys. Rev. Lett. **93**, 101801 (2004).

[15] W. W. M. Allison *et al.* (Soudan-2 Collaboration), The Atmospheric neutrino flavor ratio from a 3.9 fiducial kiloton year exposure of Soudan-2, Phys. Lett. B **449**, 137 (1999).

[16] M. Ambrosio *et al.* (MACRO Collaboration), Matter effects in upward going muons and sterile neutrino oscillations, Phys. Lett. B **517**, 59 (2001).

[17] E. Aliu *et al.* (K2K Collaboration), Evidence for muon neutrino oscillation in an accelerator-based experiment, Phys. Rev. Lett. **94**, 081802 (2005).

[18] P. Minkowski, $\mu \to e\gamma$ at a rate of one out of 10^9 muon decays?, Phys. Lett. **67B**, 421 (1977).

[19] T. Yanagida, Horizontal gauge symmetry and masses of neutrinos, Conf. Proc. C **7902131**, 95 (1979).

[20] M. Gell-Mann, P. Ramond, and R. Slansky, Complex spinors and unified theories, Conf. Proc. C **790927**, 315 (1979), arXiv:hep-th/1306.4669.

[21] S. L. Glashow, The future of elementary particle physics, NATO Sci. Ser. B **61**, 687 (1980).

[22] R. N. Mohapatra and G. Senjanovic, Neutrino mass and spontaneous parity nonconservation, Phys. Rev. Lett. **44**, 912 (1980).

[23] T. Asaka, S. Blanchet, and M. Shaposhnikov, The νMSM, dark matter and neutrino masses, Phys. Lett. B **631**, 151 (2005).

[24] T. Asaka and M. Shaposhnikov, The νMSM, dark matter and baryon asymmetry of the universe, Phys. Lett. B **620**, 17 (2005).

[25] M. Shaposhnikov and I. Tkachev, The νMSM, inflation, and dark matter, Phys. Lett. B **639**, 414 (2006).

[26] A. Kusenko, Sterile neutrinos, dark matter, and the pulsar velocities in models with a Higgs singlet, Phys. Rev. Lett. **97**, 241301 (2006).

[27] F. Bezrukov, D. Gorbunov, and M. Shaposhnikov, Late and early time phenomenology of Higgs-dependent cutoff, J. Cosmol. Astropart. Phys. 10 (2011) 001.

[28] M. Shaposhnikov, A. Shkerin, I. Timiryasov, and S. Zell, Einstein-Cartan portal to dark matter, Phys. Rev. Lett. **126**, 161301 (2021); **127**, 169901(E) (2021).

[29] J. A. Dror, D. Dunsky, L. J. Hall, and K. Harigaya, Sterile neutrino dark matter in left-right theories, J. High Energy Phys. 07 (2020) 168.

[30] K. Abazajian, G. M. Fuller, and W. H. Tucker, Direct detection of warm dark matter in the X-ray, Astrophys. J. **562**, 593 (2001).

[31] K. Abazajian, G. M. Fuller, and M. Patel, Sterile neutrino hot, warm, and cold dark matter, Phys. Rev. D **64**, 023501 (2001).

[32] A. D. Dolgov and S. H. Hansen, Massive sterile neutrinos as warm dark matter, Astropart. Phys. **16**, 339 (2002).

[33] E. Bulbul, M. Markevitch, A. Foster, R. K. Smith, M. Loewenstein, and S. W. Randall, Detection of an unidentified emission line in the stacked X-ray spectrum of galaxy clusters, Astrophys. J. **789**, 13 (2014).

[34] A. Boyarsky, O. Ruchayskiy, D. Iakubovskyi, and J. Franse, Unidentified line in X-ray spectra of the andromeda galaxy and perseus galaxy cluster, Phys. Rev. Lett. **113**, 251301 (2014).

[35] A. Boyarsky, M. Drewes, T. Lasserre, S. Mertens, and O. Ruchayskiy, Sterile neutrino dark matter, Prog. Part. Nucl. Phys. **104**, 1 (2019).

[36] M. Laine and M. Shaposhnikov, Sterile neutrino dark matter as a consequence of νMSM-induced lepton asymmetry, J. Cosmol. Astropart. Phys. 06 (2008) 031.

[37] J. Ghiglieri and M. Laine, Improved determination of sterile neutrino dark matter spectrum, J. High Energy Phys. 11 (2015) 171.

[38] M. Shaposhnikov, The νMSM, leptonic asymmetries, and properties of singlet fermions, J. High Energy Phys. 08 (2008) 008.

[39] L. Canetti, M. Drewes, T. Frossard, and M. Shaposhnikov, Dark matter, baryogenesis and neutrino oscillations from right handed neutrinos, Phys. Rev. D **87**, 093006 (2013).

[40] J. Ghiglieri and M. Laine, Sterile neutrino dark matter via coinciding resonances, J. Cosmol. Astropart. Phys. 07 (2020) 012.
[41] B. A. Campbell, J. R. Ellis, and K. A. Olive, QCD phase transitions in an effective field theory, Nucl. Phys. **B345**, 57 (1990).
[42] J. H. Applegate and C. J. Hogan, Relics of cosmic quark condensation, Phys. Rev. D **31**, 3037 (1985).
[43] J. H. Applegate, C. J. Hogan, and R. J. Scherrer, Cosmological baryon diffusion and nucleosynthesis, Phys. Rev. D **35**, 1151 (1987).
[44] K. Jedamzik, G. M. Fuller, and G. J. Mathews, Inhomogeneous primordial nucleosynthesis: Coupled nuclear reactions and hydrodynamic dissipation processes, Astrophys. J. **423**, 50 (1994).
[45] K. Jedamzik and G. M. Fuller, Nucleosynthesis in the presence of primordial isocurvature Baryon fluctuations, Astrophys. J. **452**, 33 (1995).
[46] H. Kurki-Suonio, K. Jedamzik, and G. J. Mathews, Stochastic isocurvature baryon fluctuations, baryon diffusion, and primordial nucleosynthesis, Astrophys. J. **479**, 31 (1997).
[47] M. Giovannini and M. E. Shaposhnikov, Primordial magnetic fields, anomalous isocurvature fluctuations and big bang nucleosynthesis, Phys. Rev. Lett. **80**, 22 (1998).
[48] K. Kamada and A. J. Long, Baryogenesis from decaying magnetic helicity, Phys. Rev. D **94**, 063501 (2016).
[49] K. Kamada and A. J. Long, Evolution of the baryon asymmetry through the electroweak crossover in the presence of a helical magnetic field, Phys. Rev. D **94**, 123509 (2016).
[50] V. A. Kuzmin, M. E. Shaposhnikov, and I. I. Tkachev, Matter—antimatter domains in the universe: A solution of the vacuum walls problem, Phys. Lett. **105B**, 167 (1981).
[51] A. Dolgov and J. Silk, Baryon isocurvature fluctuations at small scales and baryonic dark matter, Phys. Rev. D **47**, 4244 (1993).
[52] A. D. Dolgov, M. Kawasaki, and N. Kevlishvili, Inhomogeneous baryogenesis, cosmic antimatter, and dark matter, Nucl. Phys. **B807**, 229 (2009).
[53] S. P. Mikheev and A. Y. Smirnov, Resonant amplification of neutrino oscillations in matter and solar neutrino spectroscopy, Nuovo Cimento C **9**, 17 (1986).
[54] K. Kajantie and H. Kurki-Suonio, Bubble growth and droplet decay in the quark hadron phase transition in the early universe, Phys. Rev. D **34**, 1719 (1986).
[55] J. Ignatius, K. Kajantie, H. Kurki-Suonio, and M. Laine, Large scale inhomogeneities from the QCD phase transition, Phys. Rev. D **50**, 3738 (1994).
[56] K. Kajantie, M. Laine, K. Rummukainen, and M. E. Shaposhnikov, Is there a hot electroweak phase transition at $m_H \gtrsim m_W$?, Phys. Rev. Lett. **77**, 2887 (1996).
[57] K. Kajantie, M. Laine, K. Rummukainen, and M. E. Shaposhnikov, A nonperturbative analysis of the finite T phase transition in $\mathrm{SU}(2) \times \mathrm{U}(1)$ electroweak theory, Nucl. Phys. **B493**, 413 (1997).
[58] K. Kajantie, M. Laine, K. Rummukainen, and M. E. Shaposhnikov, Generic rules for high temperature dimensional reduction and their application to the standard model, Nucl. Phys. **B458**, 90 (1996).
[59] M. D'Onofrio and K. Rummukainen, Standard model cross-over on the lattice, Phys. Rev. D **93**, 025003 (2016).
[60] F. Csikor, Z. Fodor, and J. Heitger, Endpoint of the hot electroweak phase transition, Phys. Rev. Lett. **82**, 21 (1999).
[61] Y. Aoki, F. Csikor, Z. Fodor, and A. Ukawa, The endpoint of the first order phase transition of the SU(2) gauge Higgs model on a four-dimensional isotropic lattice, Phys. Rev. D **60**, 013001 (1999).
[62] Y. Aoki, G. Endrodi, Z. Fodor, S. D. Katz, and K. K. Szabo, The order of the quantum chromodynamics transition predicted by the standard model of particle physics, Nature (London) **443**, 675 (2006).
[63] A. Bazavov *et al.*, Equation of state and QCD transition at finite temperature, Phys. Rev. D **80**, 014504 (2009).
[64] S. Borsanyi, G. Endrodi, Z. Fodor, A. Jakovac, S. D. Katz, S. Krieg, C. Ratti, and K. K. Szabo, The QCD equation of state with dynamical quarks, J. High Energy Phys. 11 (2010) 077.
[65] S. Borsanyi, Z. Fodor, C. Hoelbling, S. D. Katz, S. Krieg, and K. K. Szabo, Full result for the QCD equation of state with $2 + 1$ flavors, Phys. Lett. B **730**, 99 (2014).
[66] T. Bhattacharya *et al.*, QCD phase transition with chiral quarks and physical quark masses, Phys. Rev. Lett. **113**, 082001 (2014).
[67] T. Kalaydzhyan and E. Shuryak, Gravity waves generated by sounds from big bang phase transitions, Phys. Rev. D **91**, 083502 (2015).
[68] A. Neronov, A. Roper Pol, C. Caprini, and D. Semikoz, NANOGrav signal from magnetohydrodynamic turbulence at the QCD phase transition in the early Universe, Phys. Rev. D **103**, 041302 (2021).
[69] C. Caprini, R. Durrer, and X. Siemens, Detection of gravitational waves from the QCD phase transition with pulsar timing arrays, Phys. Rev. D **82**, 063511 (2010).
[70] E. Witten, Cosmic separation of phases, Phys. Rev. D **30**, 272 (1984).
[71] K. Jedamzik and G. M. Fuller, Baryon number transport in a cosmic QCD-phase transition, Nucl. Phys. **B441**, 215 (1995).
[72] M. Laine and Y. Schroder, Quark mass thresholds in QCD thermodynamics, Phys. Rev. D **73**, 085009 (2006).
[73] J. B. Rehm and K. Jedamzik, Big bang nucleosynthesis with matter/antimatter domains, Phys. Rev. Lett. **81**, 3307 (1998).
[74] L. Canetti, M. Drewes, and M. Shaposhnikov, Sterile neutrinos as the origin of dark and baryonic matter, Phys. Rev. Lett. **110**, 061801 (2013).
[75] S. Eijima, M. Shaposhnikov, and I. Timiryasov, Freeze-in and freeze-out generation of lepton asymmetries after baryogenesis in the νMSM, J. Cosmol. Astropart. Phys. 04 (2022) 049.
[76] M. M. Wygas, I. M. Oldengott, D. Bödeker, and D. J. Schwarz, Cosmic QCD epoch at nonvanishing lepton asymmetry, Phys. Rev. Lett. **121**, 201302 (2018).
[77] D. J. Schwarz and M. Stuke, Lepton asymmetry and the cosmic QCD transition, J. Cosmol. Astropart. Phys. 11 (2009) 025; 10 (2010) E01.

[78] M. M. Middeldorf-Wygas, I. M. Oldengott, D. Bödeker, and D. J. Schwarz, Cosmic QCD transition for large lepton flavor asymmetries, Phys. Rev. D **105**, 123533 (2022).
[79] D. Notzold and G. Raffelt, Neutrino dispersion at finite temperature and density, Nucl. Phys. **B307**, 924 (1988).
[80] T. Asaka, M. Laine, and M. Shaposhnikov, On the hadronic contribution to sterile neutrino production, J. High Energy Phys. 06 (**2006**) 053.
[81] T. Asaka, M. Laine, and M. Shaposhnikov, Lightest sterile neutrino abundance within the νMSM, J. High Energy Phys. 01 (2007) 091; 02 (2015) 028(E).
[82] K. Zarembo, Lepton asymmetry of the universe and charged quark gluon plasma, Phys. Lett. B **493**, 375 (2000).
[83] A. G. Cohen, D. B. Kaplan, and A. E. Nelson, Progress in electroweak baryogenesis, Annu. Rev. Nucl. Part. Sci. **43**, 27 (1993).
[84] V. A. Kuzmin, V. A. Rubakov, and M. E. Shaposhnikov, On the anomalous electroweak baryon number nonconservation in the early universe, Phys. Lett. **155B**, 36 (1985).
[85] M. E. Shaposhnikov, Possible appearance of the baryon asymmetry of the universe in an electroweak theory, JETP Lett. **44**, 465 (1986) [Pis'ma Zh. Eksp. Teor. Fiz. **44**, 364 (1986)].
[86] M. E. Shaposhnikov, Baryon asymmetry of the universe in standard electroweak theory, Nucl. Phys. **B287**, 757 (1987).
[87] R. Omnes, Possibility of matter-antimatter separation at high temperature, Phys. Rev. Lett. **23**, 38 (1969).
[88] R. Omnes, The possible role of elementary particle physics in cosmology, Phys. Rep. **3**, 1 (1972).
[89] A. Cisneros, Baryon-antibaryon phase transition at high temperature, Phys. Rev. D **7**, 362 (1973).
[90] A. D. Dolgov, NonGUT baryogenesis, Phys. Rep. **222**, 309 (1992).
[91] A. De Rujula, Avatars of a matter-antimatter universe, in *32nd Rencontres de Moriond: High-Energy Phenomena in Astrophysics* (1997), pp. 363–378, arXiv:astro-ph/9705045.
[92] O. Ruchayskiy, V. Syvolap, and R. Wursch, Lepton number survival in the cosmic neutrino background, Phys. Rev. D **108**, 123503 (2023).
[93] E. O. Nadler *et al.* (DES Collaboration), Milky Way Satellite Census. III. Constraints on dark matter properties from observations of Milky Way satellite galaxies, Phys. Rev. Lett. **126**, 091101 (2021).
[94] W. Enzi *et al.*, Joint constraints on thermal relic dark matter from strong gravitational lensing, the Ly α forest, and milky way satellites, Mon. Not. R. Astron. Soc. **506**, 5848 (2021).
[95] I. A. Zelko, T. Treu, K. N. Abazajian, D. Gilman, A. J. Benson, S. Birrer, A. M. Nierenberg, and A. Kusenko, Constraints on sterile neutrino models from strong gravitational lensing, Milky Way satellites, and the Lyman-α forest, Phys. Rev. Lett. **129**, 191301 (2022).
[96] M. R. Lovell, Anticipating the XRISM search for the decay of resonantly produced sterile neutrino dark matter, Mon. Not. R. Astron. Soc. **524**, 6345 (2023).
[97] S. Y. Khlebnikov, Fluctuation-dissipation formula for bubble wall velocity, Phys. Rev. D **46**, R3223 (1992).
[98] E. K. Akhmedov, Matter effects in oscillations of neutrinos traveling short distances in matter, Phys. Lett. B **503**, 133 (2001).
[99] O. Yasuda, Vacuum mimicking phenomena in neutrino oscillations, Phys. Lett. B **516**, 111 (2001).
[100] A. Roy and M. Shaposhnikov, Resonant production of the sterile neutrino dark matter and fine-tunings in the neutrino minimal standard model, Phys. Rev. D **82**, 056014 (2010).
[101] A. Boyarsky, O. Ruchayskiy, and M. Shaposhnikov, The role of sterile neutrinos in cosmology and astrophysics, Annu. Rev. Nucl. Part. Sci. **59**, 191 (2009).
[102] S. Alekhin *et al.*, A facility to search for hidden particles at the CERN SPS: The SHiP physics case, Rep. Prog. Phys. **79**, 124201 (2016).